Acta Crystallographica Section C
Crystal Structure Communications
ISSN 0108-2701

Supramolecular hydrogen bonding of [5,10,15,20-tetrakis(4-carboxyphenyl)-porphyrinato]palladium(II) in the presence of competing solvents

Sophia Lipstman and Israel Goldberg*

School of Chemistry, Sackler Faculty of Exact Sciences, Tel-Aviv University, Ramat-Aviv, 69978 Tel-Aviv, Israel
Correspondence e-mail: goldberg@post.tau.ac.il

Received 20 November 2007
Accepted 26 November 2007
Online 14 December 2007

The title porphyrin compound forms hydrogen-bonded adducts with methanol (1:1), $[Pd(C_{48}H_{28}N_4O_8)]\cdot CH_4O$, (I), and with water and *N*,*N*-dimethylformamide (1:4:4), $[Pd(C_{48}H_{28}N_4O_8)]\cdot 4C_3H_7NO\cdot 4H_2O$, (II). In (I), the metalloporphyrin unit lies across a mirror plane in *Cmca*, while in (II), this unit lies across an inversion center in $P\overline{1}$. Extended supramolecular hydrogen-bonded arrays are formed in (I) by intermolecular interactions between the carboxylic acid functions, either directly or through the methanol species. These layers have a wavy topology and large interporphyrin pores, which are filled in the crystal structure by double interpenetration as well as enclathration of additional non-interacting nitrobenzene solvent molecules. The supramolecular aggregation in (II) can be characterized by cascaded porphyrin layers, wherein adjacent porphyrin molecules are hydrogen bonded to one another through molecules of water that are incorporated into the hydrogen-bonding scheme. Molecules of dimethylformamide partly solvate the carboxylic acid groups and fill the interporphyrin space in the crystal structure.

Comment

Metalloporphyrin macrocycles when tetrasubstituted with 4-carboxyphenyl groups at their *meso* positions (*M*-TCPP) provide a classical example of an organic species with multiple complementary terminal functional groups directed at four diverging directions of the equatorial molecular plane, which exhibit high a propensity for self-assembling into flat hydrogen-bonded two-dimensional nets (Goldberg, 2005, and references therein). It has been shown that the carboxylic acid functions may engage readily in two different supramolecular synthons, either catemeric (chain-type) or cyclic dimeric. In the latter case, utilization of four head-to-head $(COOH)_2$ cyclic dimeric associations to four neighboring porphyrin units leads to the formation of quadrangular grid arrays with large pores (Dastidar *et al.*, 1996; Diskin-Posner & Goldberg, 1999; George & Goldberg, 2006; George *et al.*, 2006; Lipstman, Muniappan & Goldberg, 2007). In the solid, these pores are filled either by a guest template or by self-interpenetration of the networks. Every molecule of the tetraacid within such supramolecular layered assembly is involved simultaneously in eight nearly linear O—H···O interactions or four $(COOH)_2$ $R_2^2(8)$-type (Etter, 1990; Bernstein *et al.*, 1995) synthons.

In non-interwoven structures, the two-dimensional multiporphyrin layers form offset stacks along the normal direction, held together by van der Waals forces. In addition to supramolecular isomerism of the catenane type (occurrence of interwoven *versus* non-interpenetrating networks), conformational isomerism, where arrays of identical composition reveal different grid shapes, has also been observed in these systems (George *et al.*, 2006). The neat networking of the *M*-TCPP units into homogeneous multiporphyrin nets can be readily disrupted by competing solvation that can modify or prevent supramolecular association. This is common with strong Lewis base reagents, *e.g.* dimethyl sulfoxide and pyridine, which each have a higher proton affinity than the carbonyl fragments of the carboxylic acid (Lipstman *et al.*, 2006; George *et al.*, 2006). Correspondingly, the actual outcome of a given supramolecular synthesis with the *M*-TCPP building blocks *via* hydrogen bonding is not always predictable.

In the above context, we describe here the structures of the solid products, (I) and (II) (Fig. 1), obtained by crystallizing Pd-TCPP from, respectively, (i) a mixture of methanol (used to dissolve the porphyrin) and nitrobenzene (an inert reagent that commonly fills effectively intra-lattice voids in porphyrin framework solids), and (ii) a mixture of methanol and *N*,*N*-dimethylformamide (DMF).

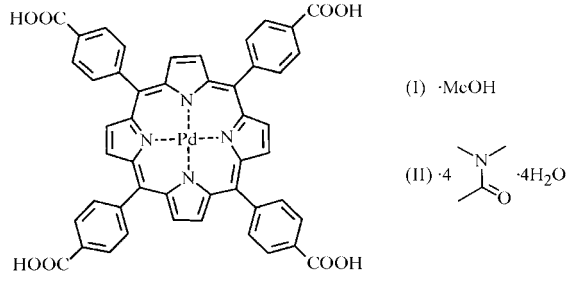

In the presence of alcohols (although they represent relatively weak hydrogen-bond donors and acceptors), the supramolecular hydrogen bonding of organic carboxylic acids does not always preserve the $(COOH)_2$ intermolecular synthon. On some occasions, incorporation of the hydroxy group into the intermolecular hydrogen-bonding scheme has been observed (Dale *et al.*, 2004). Not surprisingly, the same phenomenon characterizes the hydrogen-bonded assembly in (I). Two *cis*-related carboxylic acid groups of Pd-TCPP are involved in $R_2^2(8)$ direct-interaction synthons (Fig. 2*a*) with the carboxylic acid functions of neighboring species. However, the two other carboxylic acid residues bind to their neighbors *via* the $R_3^3(10)$ synthon (Fig. 2*b*), in which there is one methanol

 DOI: 10.1107/S0108270107063524

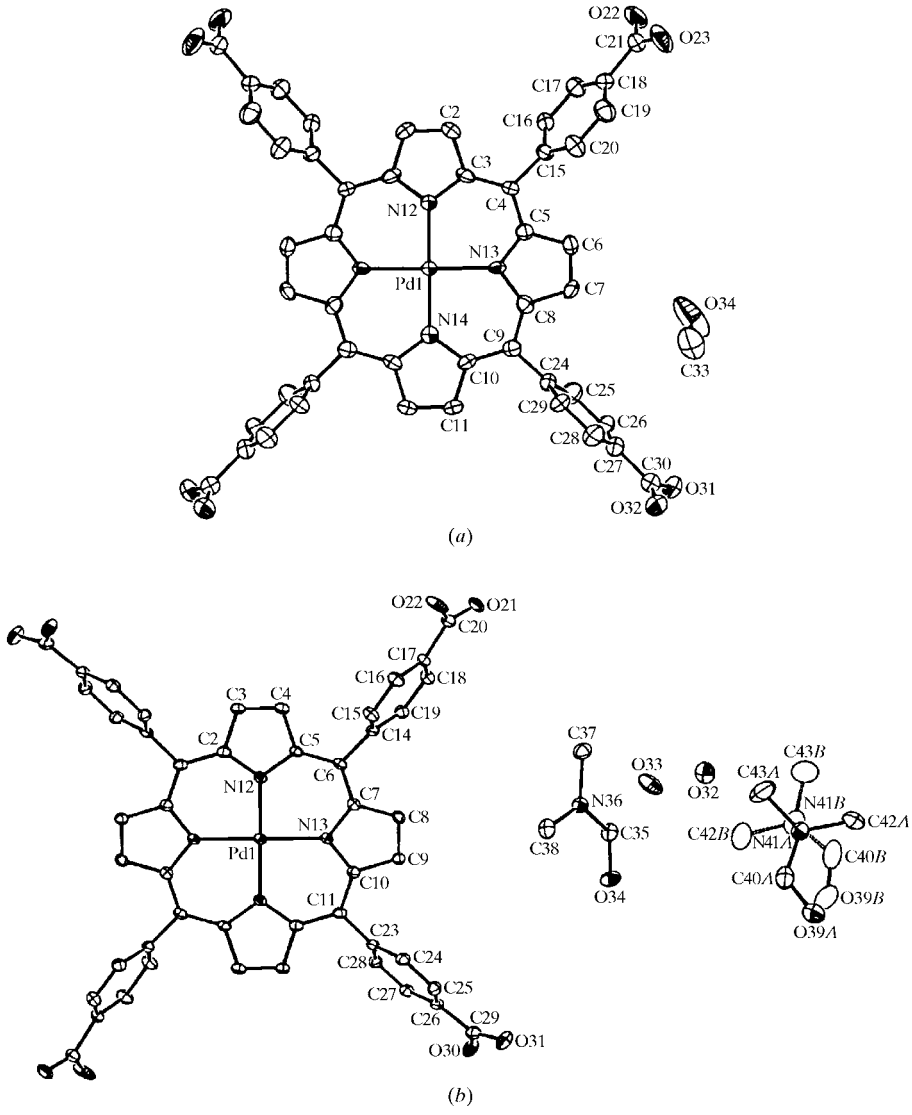

Figure 1
The molecular structure of (*a*) compound (I) and (*b*) compound (II), showing the atom-labeling schemes. Atomic ellipsoids represent displacement parameters at the 50% probability level at *ca* 110 K. H atoms have been omitted.

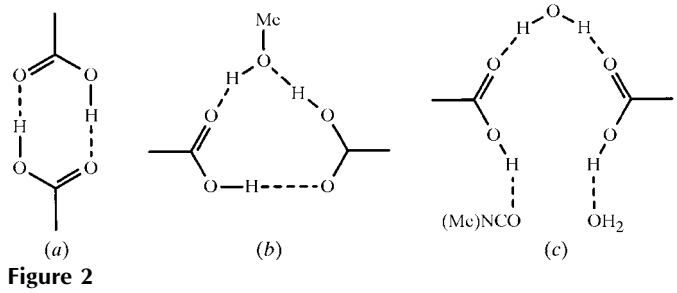

Figure 2
Schematic representations of the different hydrogen-bonding synthons between the carboxylic acid substituents. (*a*) The $R_2^2(8)$ pattern encountered in a variety of TCPP-based hydrogen-bonded networks (Dastidar *et al.*, 1996; Diskin-Posner & Goldberg, 1999; George & Goldberg, 2006; George *et al.*, 2006; Lipstman, Muniappan & Goldberg, 2007). (*b*) The $R_3^3(10)$ pattern observed in (I). (*c*) The solvation pattern of the carboxylic acid groups in (II) (see *Comment*).

molecule inserted between the two carboxylic acid groups (Table 1). This modification maintains a continuous hydrogen-bonding pattern throughout the crystal structure, where every porphyrin unit is interacting with four different neighboring species.

Evidently, in the present case, the hydrogen-bonded networks thus formed are no longer flat. Rather, they adopt a wavy shape, as illustrated in Fig. 3. While intermolecular aggregation *via* the $(COOH)_2$ bonds is associated with coplanarity of the interacting components, that *via* the COOH(MeOH)COOH $R_3^3(10)$ synthons effects a nearly perpendicular orientation of the species involved. Thus, in the observed assemblies there is a strong kink either up or down every two rows of the interlinked Pd-TCPP units. The supramolecular networks are characterized by wide interporphyrin voids. These voids are filled in the solid phase by double interpenetration, as well as by incorporation into the structure of nitrobenzene from the solvent mixture. The crystal packing of (I) is illustrated in Fig. 4. It is further stabilized by stacking interactions at an interplanar distance of approximately 4 Å between parallel porphyrin segments of the interwoven networks.

The disruption of the interporphyrin hydrogen-bonding scheme is much more severe in (II). Here, the two carboxylic acid groups of adjacent porphyrin species are solvated by two molecules of water and one molecule of DMF. One of the water molecules (atom O33) bridges by hydrogen bonding between two adjacent carbonyl fragments (atoms O21 and O31), while the other water molecule (O32) and the DMF molecule (O34 through C38) serve as H-atom acceptors from the two adjacent hydroxy residues O30 and O22 (Fig. 2*c* and Table 2). Moreover, every porphyrin unit connects *via* the first water molecule only to two neighboring porphyrins (and not to four neighbors as in the preceding example), giving rise to the formation of hydrogen-bonded one-dimensional chains as the primary supramolecular motif with coplanar porphyrin components (Fig. 5). These chain motifs further interconnect by hydrogen bonding between the O32 and O33 sites of adjacent chains, yielding an extended two-dimensional hydrogen-bonded pattern in the crystal structure, which propagates parallel to the (011) plane (Fig. 5 and Table 2). The observed hydrogen-bonding scheme corresponds (when the side hydrogen bonds to the DMF molecules are ignored) to the $C_3^3(8)$ graph-set representation. The packing arrangement of (II) is shown in Fig. 6. The porphyrin frameworks displaced

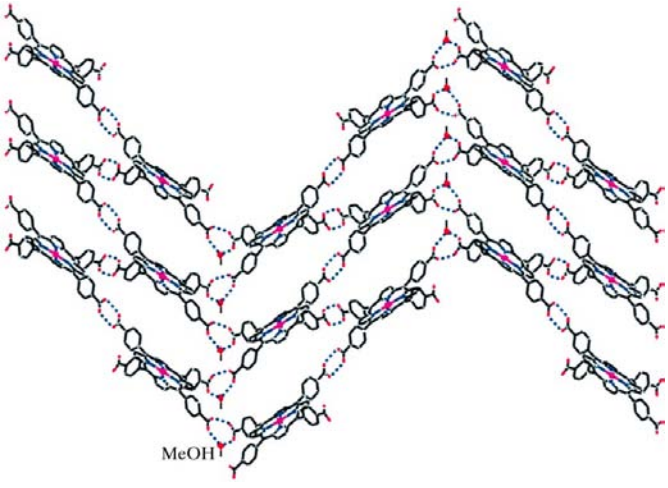

Figure 3
The supramolecular hydrogen-bonded wavy layers in (I). Hydrogen bonds are marked by dotted lines. The palladium ions and methanol O atoms are indicated by small spheres. H atoms are not shown.

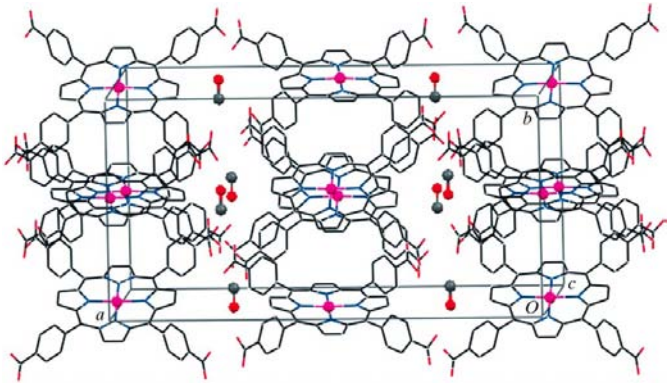

Figure 4
The crystal structure of (I). The palladium ions and methanol molecule are indicated by small spheres. H atoms and the disordered nitrobenzene solvent molecule have been omitted.

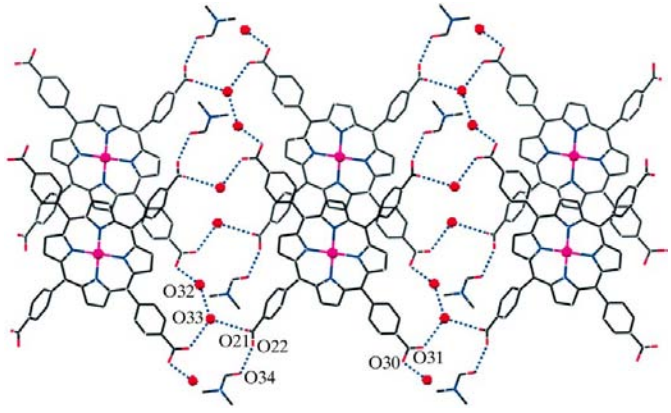

Figure 5
Illustration of the supramolecular hydrogen bonding in (II). The Pd atoms and water molecules are indicated by small spheres. Hydrogen bonds are marked by dotted lines. The disordered DMF molecule and the H atoms have been omitted. Crystallographic translation along *a* relates the two shown rows of the porphyrin molecules. Atomic labels identify the O atoms (or their symmetry equivalents) that are involved in the hydrogen bonds.

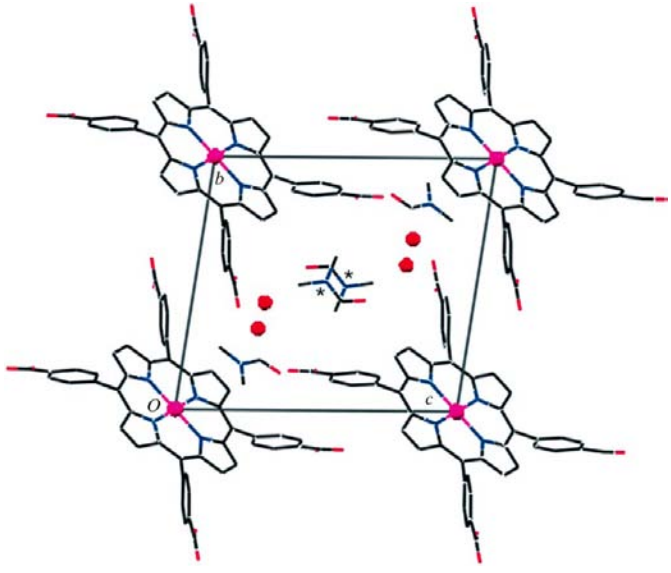

Figure 6
The crystal packing of (II), projected down the *a* axis. Pd atoms and water molecules are indicated by spheres. The disordered DMF species located between neighboring hydrogen-bonded layers (only a single orientation of each is shown) are marked by asterisks. They reside near $x = 0.26$, $y = 0.51$, $z = 0.45$, filling the interporphyrin space.

along the *a* axis are arranged in an offset stacked manner with a minor overlap between adjacent molecules along the stack and an average spacing of about 4.6 Å. Additional molecules of the DMF solvent are included in the interface between the hydrogen-bonded layers centered at $z = 0$ and $z = 1$ in a disordered manner (fragments O39*A*–C43*A* and O39*B*–C43*B*). They form hydrogen bonds to the O32 water molecule.

In summary, this study describes the effects of competing solvation on the self assembly of TCPP-type porphyrin building blocks by hydrogen bonding, where solvent components with comparable H-atom donating or accepting capacity interfere with direct assembly of the porphyrin units into homogeneous single-component arrays. It should be noted that Pd-TCPP and related metalloporphyrins are also excellent building blocks for networking through external metal ion bridging auxiliaries, which can coordinate to the peripheral carboxylic acid groups, and yield by multiple coordination robust supramolecular arrays (Goldberg, 2005, and references therein; Shmilovits *et al.*, 2003; Lipstman, Muniappan, George & Goldberg, 2007).

Experimental

Pd-TCPP was obtained commercially from Porphyrin Systems GbR. Compound (I) was obtained by dissolving the metalloporphyrin (2.7 mg, 0.003 mmol) in a minimal amount of methanol. To this, six drops of nitrobenzene were added. Slow evaporation of the resulting mixture yielded, after one month, X-ray quality red rhombus-like crystals. Reaction of Pd-TCPP (2 mg, 0.002 mmol) with a minimal amount of methanol and a few drops of DMF yielded crystals of (II) under otherwise similar crystallization conditions.

Compound (I)

Crystal data

$[Pd(C_{48}H_{28}N_4O_8)]\cdot CH_4O$
$M_r = 927.21$
Orthorhombic, *Cmca*
$a = 31.0347$ (6) Å
$b = 15.9441$ (11) Å
$c = 18.3824$ (7) Å
$V = 9096.0$ (7) Å^3
$Z = 8$
Mo $K\alpha$ radiation
$\mu = 0.47$ mm^{-1}
$T = 110$ (2) K
0.30 × 0.10 × 0.05 mm

Data collection

Nonius KappaCCD diffractometer
20365 measured reflections
4344 independent reflections
2688 reflections with $I > 2\sigma(I)$
$R_{int} = 0.098$

Refinement

$R[F^2 > 2\sigma(F^2)] = 0.070$
$wR(F^2) = 0.160$
$S = 1.00$
4344 reflections
291 parameters
12 restraints
H-atom parameters constrained
$\Delta\rho_{max} = 0.50$ e Å^{-3}
$\Delta\rho_{min} = -0.77$ e Å^{-3}

Table 1
Hydrogen-bond geometry (Å, °) for (I).

D—H···A	D—H	H···A	D···A	D—H···A
O23—H23···O23^{i}	0.84	1.84	2.542 (9)	141
O31—H31···O32^{ii}	0.89	1.77	2.669 (6)	180
O34—H34···O22^{iii}	0.90	1.71	2.608 (7)	179

Symmetry codes: (i) $-x+\frac{1}{2}, y, -z+\frac{3}{2}$; (ii) $-x+\frac{1}{2}, -y-\frac{1}{2}, -z$; (iii) $-x+\frac{1}{2}, -y+\frac{1}{2}, -z+1$.

Compound (II)

Crystal data

$[Pd(C_{48}H_{28}N_4O_8)]\cdot 4C_3H_7NO\cdot 4H_2O$
$M_r = 1259.61$
Triclinic, $P\overline{1}$
$a = 7.7243$ (2) Å
$b = 13.2668$ (4) Å
$c = 14.5878$ (5) Å
$\alpha = 81.3820$ (16)°
$\beta = 87.3282$ (17)°
$\gamma = 87.0384$ (17)°
$V = 1474.91$ (8) Å^3
$Z = 1$
Mo $K\alpha$ radiation
$\mu = 0.39$ mm^{-1}
$T = 110$ (2) K
0.60 × 0.10 × 0.10 mm

Data collection

Nonius KappaCCD diffractometer
12855 measured reflections
5498 independent reflections
4868 reflections with $I > 2\sigma(I)$
$R_{int} = 0.045$

Refinement

$R[F^2 > 2\sigma(F^2)] = 0.037$
$wR(F^2) = 0.083$
$S = 1.02$
5498 reflections
437 parameters
8 restraints
H-atom parameters constrained
$\Delta\rho_{max} = 0.31$ e Å^{-3}
$\Delta\rho_{min} = -0.72$ e Å^{-3}

Table 2
Hydrogen-bond geometry (Å, °) for (II).

D—H···A	D—H	H···A	D···A	D—H···A
O22—H22···O34^{i}	0.95	1.57	2.516 (2)	173
O30—H30···O32^{ii}	0.99	1.59	2.543 (3)	161
O32—H32*A*···O39*B*^{iii}	0.91	1.74	2.642 (4)	170
O32—H32*A*···O39*A*^{iii}	0.91	1.91	2.799 (5)	164
O32—H32*B*···O33	0.97	1.75	2.714 (3)	177
O33—H33*A*···O21^{iv}	0.91	1.87	2.776 (3)	169
O33—H33*B*···O31^{iii}	0.91	1.89	2.773 (3)	166

Symmetry codes: (i) $x-2, y, z$; (ii) $-x+2, -y+1, -z+1$; (iii) $-x+1, -y+1, -z+1$; (iv) $x+1, y, z$.

H atoms bound to C atoms were located in calculated positions and were constrained to ride on their parent atoms, with C—H distances of 0.95 and 0.98 Å, and with U_{iso}(H) values of 1.2 or 1.5 times U_{eq}(C). H atoms bound to O atoms were either located in difference Fourier maps or placed in calculated positions to correspond to idealized hydrogen-bonding geometries, with O—H distances within the range 0.84–0.99 Å. Their atomic positions were not refined, and they were constrained to ride on their parent atoms with U_{iso}(H) values of 1.2 times U_{eq}(O). In (I), the porphyrin and methanol components are located on mirror planes and twofold axes, respectively. The hydrogen-bonding scheme is characterized by a twofold disorder about the rotation axes. Correspondingly, the methanol molecule and the carboxylic acid groups also exhibit partial disorder. The nitrobenzene solvent molecule incorporated into the crystal structure of (I) is also positioned on, and severely disordered about, the ($\frac{1}{2}yz$) mirror plane, being centered approximately at ($\frac{1}{2}$, 0.1, 0.4). It could not be reliably modeled by discrete atoms. Correspondingly, its contribution was subtracted from the diffraction data by the SQUEEZE procedure (*PLATON*; Spek, 2003). In (II), one of the DMF species (O39/C40/N41/C42/C43) exhibits a twofold orientational disorder, which could be modeled, and it was refined with restrained geometry in order to avoid irregular values for bond lengths and bond angles. The Pd-TCPP reference unit is located on an inversion center at (0, 0, 1).

For both compounds, data collection: *COLLECT* (Nonius, 1999); cell refinement: *DENZO* (Otwinowski & Minor, 1997); data reduction: *DENZO* and *SCALEPACK* (Otwinowski & Minor, 1997);

program(s) used to solve structure: *SIR97* (Altomare *et al.*, 1999); program(s) used to refine structure: *SHELXL97* (Sheldrick, 1997); molecular graphics: *ORTEPIII* (Burnett & Johnson, 1996) and *Mercury* (Macrae *et al.*, 2006); software used to prepare material for publication: *SHELXL97*.

This research was supported in part by The Israel Science Foundation.

Supplementary data for this paper are available from the IUCr electronic archives (Reference: GD3172). Services for accessing these data are described at the back of the journal.

References

Altomare, A., Burla, M. C., Camalli, M., Cascarano, G. L., Giacovazzo, C., Guagliardi, A., Moliterni, A. G. G., Polidori, G. & Spagna, R. (1999). *J. Appl. Cryst.* **32**, 115–119.

Bernstein, J., Davis, R. E., Shimoni, L. & Chang, N.-L. (1995). *Angew. Chem. Int. Ed. Engl.* **34**, 1555–1575.

Burnett, M. N. & Johnson, C. K. (1996). *ORTEPIII*. Report ORNL-6895. Oak Ridge National Laboratory, Tennessee, USA.

Dale, S. H., Elsegood, M. R. J. & Richards, S. G. (2004). *Chem. Commun.* pp. 1278–1279.

Dastidar, P., Stein, Z., Goldberg, I. & Strouse, C. E. (1996). *Supramol. Chem.* **7**, 257–270.

Diskin-Posner, Y. & Goldberg, I. (1999). *Chem. Commun.* pp. 1961–1962.

Etter, M. C. (1990). *Acc. Chem. Res.* **23**, 120–126.

George, S. & Goldberg, I. (2006). *Cryst. Growth Des.* **6**, 755–762.

George, S., Lipstman, S., Muniappan, S. & Goldberg, I. (2006). *CrystEngComm*, **8**, 417–424.

Goldberg, I. (2005). *Chem. Commun.* pp. 1243–1254.

Lipstman, S., Muniappan, S., George, S. & Goldberg, I. (2006). *CrystEngComm*, **8**, 601–607.

Lipstman, S., Muniappan, S., George, S. & Goldberg, I. (2007). *Dalton Trans.* pp. 3273–3281.

Lipstman, S., Muniappan, S. & Goldberg, I. (2007). *Acta Cryst.* C**63**, o371–o373.

Macrae, C. F., Edgington, P. R., McCabe, P., Pidcock, E., Shields, G. P., Taylor, R., Towler, M. & van de Streek, J. (2006). *J. Appl. Cryst.* **39**, 453–457.

Nonius, B. V. (1999). *COLLECT*. Nonius BV, Delft, The Netherlands.

Otwinowski, Z. & Minor, W. (1997). *Methods in Enzymology*, Vol. 276, *Macromolecular Crystallography*, Part A, edited by C. W. Carter Jr & R. M. Sweet, pp. 307–326. New York: Academic Press.

Sheldrick, G. M. (1997). *SHELXL97*. University of Göttingen, Germany.

Shmilovits, M., Diskin-Posner, Y., Vinodu, M. & Goldberg, I. (2003). *Cryst. Growth Des.* **5**, 855–863.

Spek, A. L. (2003). *J. Appl. Cryst.* **36**, 7–13.